Brazilian Journal of Chemical Engineering (2023) 40:231–245
https://doi.org/10.1007/s43153-022-00238-2

ORIGINAL PAPER

Design of double pipe heat exchanger structures using linear models and smart enumeration

Alice Peccini[1,2] · Miguel J. Bagajewicz[1,2,3] · André L. H. Costa[2]

Received: 16 September 2021 / Revised: 26 February 2022 / Accepted: 6 March 2022 / Published online: 8 April 2022

Abstract

The design of double pipe heat exchanger hairpin-based structures has been presented in the form of a mixed-integer nonlinear model (MINLM). While some metaheuristics/stochastic methods can provide good answers, the only way to guarantee global solutions of this model is by using mixed-integer nonlinear programming (MINLP). Our novel contribution focuses on globally optimal solutions obtained robustly, that is, without convergence and initialization issues. For that purpose, as an alternative to the direct solution of the original nonlinear mathematical model, we propose the use of a rigorous linear reformulation of a MINLM to a linear model (MILM). Because the reformulation is rigorous, the global optimum of the original nonlinear model is obtained using a MILP approach. Smart enumeration procedures, applicable after parametrization of the search space are applied to overcome computational obstacles associated with solving the reformulation resultant MILP. Our approach presents various novelties: parametrization, calculation of lower bounds, and Smart Enumeration, a recently introduced technique, extendable to the solution of other problems. Numerical examples illustrate the corresponding performances.

Keywords Optimization · Double pipe heat exchanger · Design · Mixed-integer linear programming

List of symbols

Parameters

$\widehat{\Delta P}_{sST_{disp}}$	Available pressure drop (Pa)
$\widehat{\Delta Tlm}$	Logarithmic mean temperature difference (K)
$\widehat{\mu}_{sST}$	Viscosity (Pa·s)
$\widehat{\rho}_{sST}$	Density (kg/m^3)
$\widehat{A}_{exc}$	Minimum area excess (%)
$\widehat{Cp}_{sST}$	Heat capacity (J/(kg K))
$\widehat{k}_{sST}$	Thermal conductivity (W/(m°C))
$\widehat{ktube}$	Tube thermal conductivity (W/m°C)
$\widehat{m}_{sST}$	Mass flow rate (kg/s)
$\widehat{pA}_{sd,sB,sE,sNh,sLh,sE'}$	Heat exchanger area (m^2)
$\widehat{pAa}_{sd,sD}$	Annular region area (m^2)
$\widehat{pdh}_{sd,sD}$	Hydraulic diameter (m)
$\widehat{pdte}_{sd}$	Inside tube external diameter (m)
$\widehat{pDte}_{sD}$	Outside tube external diameter (m)
$\widehat{pdti}_{sd}$	Inside tube internal diameter (m)
$\widehat{pDti}_{sD}$	Outside tube internal diameter (m)
$\widehat{pdPa1}_{sd,sD,sB,sE,sNh,sLh,sE',sST}$	Pressure drop parameter
$\widehat{pdPa23}_{sd,sD,sB,sE,sNh,sLh,sE',sST}$	Pressure drop parameter
$\widehat{pdPa4}_{sd,sD,sB,sE,sNh,sLh,sE',sST}$	Pressure drop parameter
$\widehat{pdPt1}_{sd,sB,sE,sNh,sLh,sE',sST}$	Pressure drop parameter
$\widehat{pdPt23}_{sd,sB,sE,sNh,sLh,sE',sST}$	Pressure drop parameter
$\widehat{pdPt4}_{sd,sB,sE,sNh,sLh,sE',sST}$	Pressure drop parameter
$\widehat{pF}_{sST,sE}$	F factor in case *sST* stream is in series, for $sE \neq 1$
$\widehat{pLh}_{sLh}$	Hairpin tube length (m)
$\widehat{pNB}_{sB}$	Number of branches

✉ André L. H. Costa
andrehc@uerj.br

[1] Federal University of Rio de Janeiro (UFRJ), Escola de Química CT, Bloco E, Ilha do Fundão, Rio de Janeiro, RJ CEP 21949-900, Brazil

[2] Rio de Janeiro State University (UERJ), Rua São Francisco Xavier, 524, Maracanã, Rio de Janeiro, RJ CEP 20550-900, Brazil

[3] School of Chemical, Biological and Materials Engineering, University of Oklahoma, Norman, OK 73019, USA

$\widehat{pNE}_{sE}$ Number of heat exchangers in series per branch

$\widehat{pNh}_{sNh}$ Number of available hairpins per unit

$\widehat{pNua}^{Gni}_{tran_{sd,sD,sB,sE',sST}}$ Gnielinski correlation parameter for transitional flow

$\widehat{pNut}^{Gni}_{tran_{sd,sB,sE,sST}}$ Gnielinski correlation parameter for transitional flow

$\widehat{pNua}^{Gni}_{turb_{sd,sD,sB,sE',sST}}$ Gnielinski correlation parameter for turbulent flow

$\widehat{pNut}^{Gni}_{turb_{sd,sB,sE,sST}}$ Gnielinski correlation parameter for turbulent flow

$\widehat{pNua}^{Hau}_{sd,sD,sB,sE',sLh,sST}$ Hausen correlation parameter

$\widehat{pNut}^{Hau}_{sB,sE,sLh,sST}$ Hausen correlation parameter

$\widehat{pNua}^{S\&T}_{sd,sD,sB,sE,sLh,sST}$ S&T correlation parameter

$\widehat{pNut}^{S\&T}_{sB,sE,sLh,sST}$ S&T correlation parameter

$\widehat{Q}$ Heat transfer rate (W)

$\widehat{Rf}_{sST}$ Fouling resistance (m^2°C/W)

$\widehat{Ti}_{sST}$ Inlet temperature (°C)

$\widehat{To}_{sST}$ Outlet temperature (°C)

$\widehat{va}_{max/min}$ Annulus-side velocity bounds (m/s)

$\widehat{vt}_{max/min}$ Tube-side velocity bounds (m/s)

Continuous variables

ΔPa Annulus-side pressure drop (Pa)

ΔPt Tube-side pressure drop (Pa)

A Heat transfer area (m^2)

$Nua^{S\&T}$ Annulus-side Seider & Tate Nusselt number

$Nut^{S\&T}$ Tube-side Seider & Tate Nusselt number

Pra Annulus-side stream Prandtl number

Prt Tube-side stream Prandtl number

Rea Annulus-side Reynolds number

Ret Inner tube Reynolds number

U Overall Heat Transfer Coefficient (W/m^2°C)

va Annulus-side velocity (m/s)

vt Tube-side velocity (m/s)

$wA_{sd,sB,sE,sNh,sLh,sE'}$ Replacement for $yd_{sd}yB_{sB}yPt_{sE}yNh_{sNh}yLh_{sLh}yS_{sE'}$

$wAF_{sd,sB,sNh,sLh,sE,sE',sST}$ Replacement for $wA_{sd,sB,sNh,sLh,sE,sE'}yT_{sST}$

$wdPa_{sd,sD,sB,sNh,sLh,sE,sE',sST,sRea}$ Replacement for $wA_{sd,sB,sE,sNh,sLh,sE'}yD_{sD}yT_{sST}yRea_{sRea}$

$wdPt_{sd,sB,sNh,sLh,sE,sE',sST,sRet}$ Replacement for $wA_{sd,sB,sE,sNh,sLh,sE'}yT_{sST}yRet_{sRet}$

$wha^{Gni}_{sd,sD,sB,sE',sLh,sST,sRea}$ Replacement for $wva_{sd,sD,sB,sE',sST}yLh_{sLh}yRea_{sRea}$

$wha^{Hau}_{sd,sD,sB,sE',sLh,sST,sRea,sPra}$ Replacement for $wva_{sd,sD,sB,sE',sST}yLh_{sLh}yRea_{sRea}yPra_{sPra}$

$wha^{S\&T}_{sd,sD,sB,sE',sLh,sST,sRea,sPra,sNua}$ Replacement for $wva_{sd,sD,sB,sE',sST}yLh_{sLh}yRea_{sRea}yPra_{sPra}yNua_{sNua}$

$wha^{theo}_{sd,sD,sST,sRea,sPra,sNua}$ Replacement for $wydT_{sd,sST}yD_{sD}yRea_{sRea}yPra_{sPra}yNua_{sNua}$

$wht^{Gni}_{sd,sB,sE,sST,sRet}$ Replacement for $wvt_{sd,sB,sE,sST}yRet_{sRet}$

$wht^{Hau}_{sd,sB,sE,sLh,sST,sRet,sPrt}$ Replacement for $wvt_{sd,sB,sE,sST}yLh_{sLh}yRet_{sRet}yPrt_{sPrt}$

$wht^{S\&T}_{sd,sB,sE,sLh,sST,sRet,sPrt,sNut}$ Replacement for $wvt_{sd,sB,sE,sST}yLh_{sLh}yRet_{sRet}yPrt_{sPrt}yNut_{sNut}$

$wht^{theo}_{sd,sST,sRet,sPrt,sNut}$ Replacement for $wydT_{sd,sST}yRet_{sRet}yPrt_{sPrt}yNut_{sNut}$

$wNua_{sd,sD,sB,sE,sLh,sST}$ Replacement for $wva_{sd,sD,sB,sE,sST}yLh_{sLh}$

$wNut_{sB,sE,sLh,sST}$ Replacement for $yB_{sB}yPt_{sE}yLh_{sLh}yT_{sST}$

$wva_{sd,sD,sB,sE,sST}$ Replacement for $yd_{sd}yD_{sD}yB_{sB}yPa_{sE}yT_{sST}$

$wvt_{sd,sB,sE,sST}$ Replacement for $yd_{sd}yB_{sB}yPt_{sE}yT_{sST}$

$wydT_{sd,sST}$ Replacement for $yd_{sd}yT_{sST}$

Binary variables

yB_{sB} Number of branches selection

yd_{sd} Inner tube diameter selection

yD_{sD} Outer tube diameter selection

yLh_{sLh} Hairpin tube length selection

yNh_{sNh} Number of hairpins per unit selection

$yNua_{sNua}$ Range of annular region Seider and Tate Nusselt number selection

$yNut_{sNut}$ Range of inner tube Seider and Tate Nusselt number selection

yPa_{sE} Annulus side number of units in parallel per branch selection

$yPra_{sPra}$ Range of annular region Prandtl number selection

$yPrt_{sPrt}$	Range of inner tube Prandtl number selection
yPt_{sE}	Tube-side number of units in parallel per branch selection
$yRea_{sRea}$	Range of annular region Reynolds number selection
$yRet_{sRet}$	Range of inner tube Reynolds number selection
yT_{sST}	Stream allocation

Indices

sB	Number of branches
sd	Inner tube diameters
sD	Outer tube diameters
sE	Number of units per branch
sLh	Hairpin tube length
sNh	Number of hairpins per unit
sNua	Range of annular region Seider and Tate Nusselt number
sNut	Range of inner tube Seider and Tate Nusselt number
sPra	Range of annular region Prandtl number
sPrt	Range of inner tube Prandtl number
sRea	Range of annular region Reynolds number
sRet	Range of inner tube Reynolds number
sST	Stream

Introduction

Double pipe heat exchangers can be an advantageous thermal equipment alternative in several tasks. They are the easiest heat exchangers to fabricate as well as maintain/repair, especially if they have been standardized in the form of hairpins and specific structural arrangements (series, series/parallel, etc.). They are used in small heat exchange tasks, usually limited to areas lower than 50 m^2. They are also preferred when dealing with high-pressure applications because smaller diameters than shell and tube exchangers are used. The industries involved cover a wide range: petroleum, food, refrigeration, etc. (Kakaç and Liu 2002; Guy 2008).

The literature about the design of double-pipe heat exchangers is focused on the optimization of heat transfer intensification devices, such as fins (Sahiti et al. 2008; Syed et al. 2011; Iqbal et al. 2011; Iqbal et al. 2011), corrugations (Han et al. 2015; Sruthi et al. 2021), micro-fins (Dastmalchi et al. 2017; Xie et al. 2022), and turbulence promoters (Arjmandi et al. 2020; Kumar and Dinesha 2021; Kola et al. 2021). General and optimal design of double pipe heat exchangers received the attention of fewer authors. Söylemez (2004) addressed the optimization of double pipe heat exchangers for the identification of the optimal value of the heat exchanger diameters aiming at the minimization of the total annualized cost. Swamee et al. (2008) formulated the design optimization problem using the diameters of the inner and outer tubes and the utility flow rate as design variables to minimize operational costs. Peccini et al. (2019) proposed the minimization of the heat transfer area using a mixed-integer nonlinear programming (MINLP) approach, which included different alternatives of parallel and series configurations in the search space. Although it provides good opportunities for cost reductions by finding better solutions than traditional approaches based on sucessive trials, its nonconvex nature sometimes presents convergence limitations and/or poor local optimum termination, if local solvers are used. Moloodpoor et al. (2021) employed a stochastic optimization method for the solution of a design problem similar to Swamee et al. (2008). Nahes et al. (2019) investigated the area minimization of the design of double pipe heat exchangers using mathematical programming considering the variation of the physical properties with temperature but exploring a more limited search space than Peccini et al. (2019). Textbooks (Saunders 1988; Kakaç and Liu 2002; Serth 2007) usually use traditional trial and verification procedures, where optimality is not the main goal.

This paper addresses the design optimization of double pipe heat exchangers using as a starting point the MINLP problems of Peccini et al. (2019). To circumvent the aforementioned potential difficulties of nonlinear solvers observed in Peccini et al. (2019), the current paper proposes a reformulation of the original mixed-integer nonlinear model (MINLM), resulting in a mixed-integer linear model (MILM), which we solve using a mixed-integer linear programming (MILP) procedure, thus guaranteeing a global optimum. Our reformulation does not make simplifications, approximations, or linearization of the original model, i.e. the solutions of the original MINLP are also solutions of the new MILP problem and vice versa. Limitations associated with the resultant increase of the number of variables and constraints of the linear model are handled through the proposition of alternative enumeration procedures aided by a parametrization of the search space, made possible by the discrete nature of the variables involved. Indeed, once a few variables of the problem are parametrized, the search space can be described by a set of candidates, obtained by combinations of the discrete equations turned into parameters. The candidates are then subject to an organization according to a rigorous lower bound of the objective function that we developed. The availability of this lower bound allows the acceleration of the Smart Enumeration procedure. This novel approach to handle large-size MILP problems can be employed to solve similar problems in other fields of applications.

Heat exchanger design equations

The basic structure of double pipe heat exchangers consists of two concentric tubes. The heat transfer equations, based on the LMTD method, are:

$$\hat{Q} = \hat{m}_h Cp_h(\hat{Ti}_h - \hat{To}_h) \tag{1}$$

$$\hat{Q} = \hat{m}_c Cp_c(\hat{To}_c - \hat{Ti}_c) \tag{2}$$

$$\hat{Q} = UA\widehat{\Delta Tlm} \tag{3}$$

$$\frac{1}{U} = \frac{1}{h_t}\frac{d_e}{d_i} + \widehat{Rf}_t\frac{d_e}{d_i} + \frac{d_e \ln\left(\frac{d_e}{d_i}\right)}{2\widehat{k_{tube}}} + \widehat{Rf}_a + \frac{1}{h_a} \tag{4}$$

The heat transfer coefficients (h_t, h_a) are obtained from a Nusselt number correlation (we use Gnielinski et al., Hauser et al., and Sieder and Tate) (Incropera and Dewitt 2007). Finally, ignoring minor head losses in connections and bends, the pressure drop of the flow in the inner tube is calculated by the Darcy–Weisbach equation. In turn, the annular section pressure drop is obtained using the same equation, but using hydraulic diameters (omitting the viscosity correction factor) (Saunders 1988).

$$\Delta P_t = \rho_t f_t \frac{L}{d_i}\frac{v_t^2}{2} \tag{5}$$

$$\Delta P_a = \rho_a f_a \frac{L}{dh}\frac{v_a^2}{2} \tag{6}$$

Double pipe heat exchanger hairpin architecture

Double pipe heat exchangers are usually commercialized in hairpin structures, as shown in Fig. 1a. Figure 1b illustrates three hairpins connected in series.

Different interconnection patterns among the heat exchanger hairpins provide flexible alternatives to abide by heat load and maximum pressure drop specifications of the service. In our model, a hairpin is the countercurrent basic structure; a unit is defined as multiple hairpins connected in series; a branch is a structure that can be arranged in some proposed complex series/parallel configurations (see Fig. 2), which can then be arranged in a set of parallel branches, rendering the general structure (See Fig. 3) (Peccini et al. 2019).

Linear formulation of the design problem

In a prior work (Peccini et al. 2019), a MINLM was proposed (see Supplementary Information—Section S1). Here, we show that this model can be rigorously reformulated in a linear one. The techniques employed in this transformation are described in Costa and Bagajewicz (2019).

Selection of the geometric variables

We use the following set of binary variables to describe the design variables: yd_{sd} for the inner tube diameter options (discrete options: $\widehat{pdte}_{sd}$ and $\widehat{pdti}_{sd}$), yD_{sD} for the outer tube diameter (discrete options: $\widehat{pDte}_{sd}$ and $\widehat{pDti}_{sd}$), yLh_{sLh} for the hairpin tube length (discrete options: $\widehat{pLh}_{sLh}$), yNh_{sNh} for the number of hairpins per unit (discrete options: $\widehat{pNh}_{sNh}$), yB_{sB} for the number of parallel branches present in the heat exchanger design (discrete options: $\widehat{pNB}_{sB}$), yPt_{sE} and yPa_{sE}

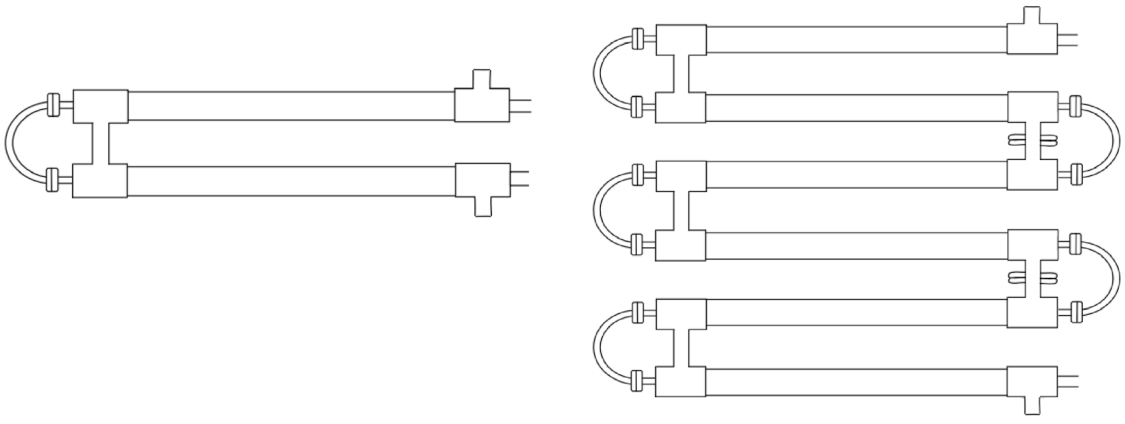

(a) Hairpin structure

(b) Three hairpins connected in series.

Fig. 1 Double pipe heat exchanger hairpin structure. **a** Hairpin structure. **b** Three hairpins connected in series

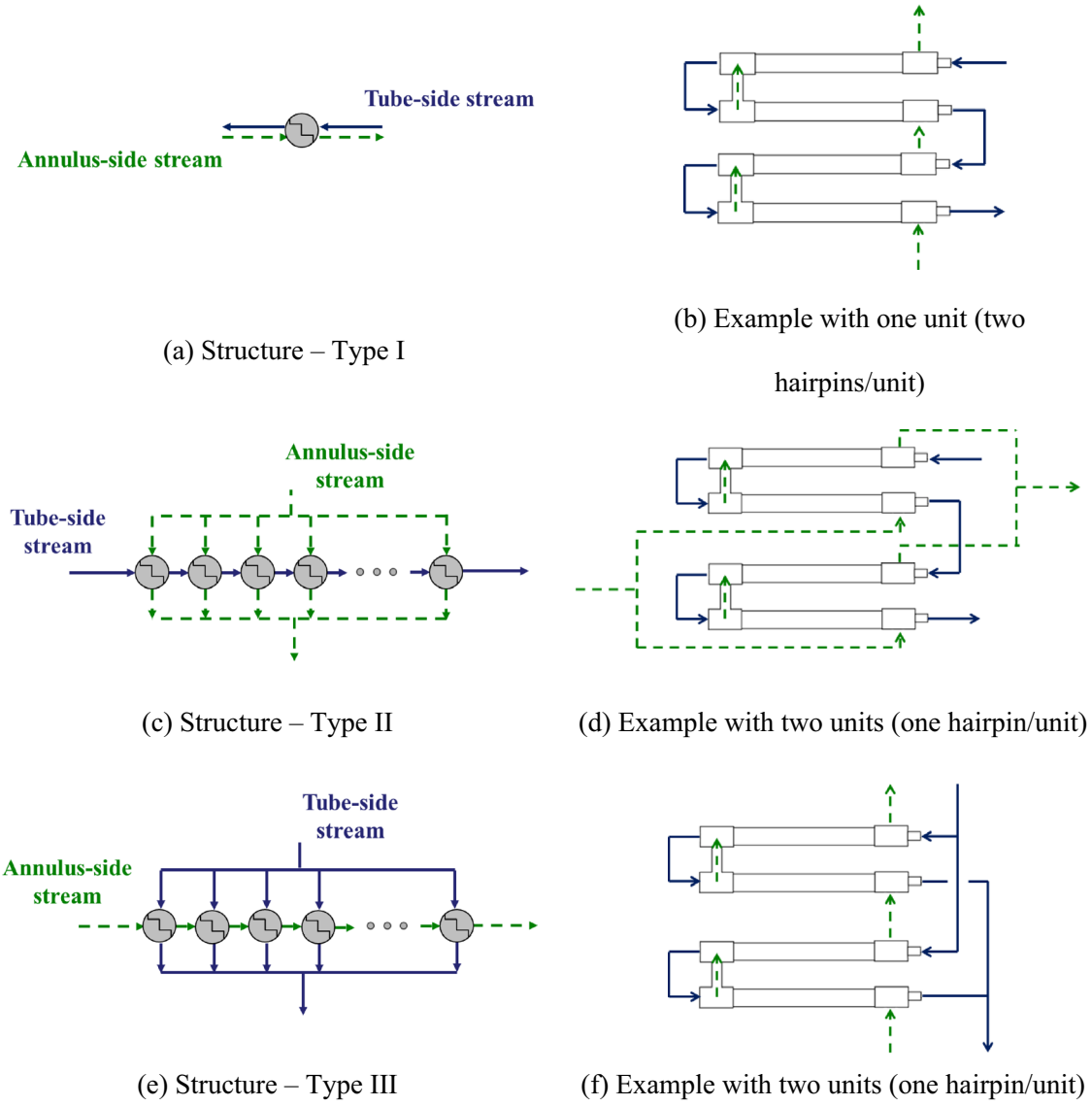

(a) Structure – Type I

(b) Example with one unit (two hairpins/unit)

(c) Structure – Type II

(d) Example with two units (one hairpin/unit)

(e) Structure – Type III

(f) Example with two units (one hairpin/unit)

Fig. 2 Different flow arrangements. **a**, **b** Type I: tube-side and annulus-side streams in series; **c**, **d** Type II: tube-side stream in series and annulus-side stream in parallel; **e**, **f** Type III: annulus-side stream in series and tube-side stream in parallel

for the number of units aligned in parallel in each branch for the tube-side and the annulus-side streams (discrete options: $\widehat{pNE}_{sE}$).

This set of binary variables must be associated with constraints to ensure that only one of the available options will be selected:

$$\sum_{sd=1}^{sdmax} yd_{sd} = \sum_{sD=1}^{sDmax} yD_{sD} = \sum_{sLh=1}^{sLhmax} yLh_{sLh} = \sum_{sNh=1}^{sNhmax} yNh_{sNh} = \sum_{sB=1}^{sBmax} yB_{sB} = \sum_{sE=1}^{sEmax} yPt_{sE} = \sum_{sE=1}^{sEmax} yPa_{sE} = 1 \quad (7)$$

Stream allocation

The allocation of streams is controlled by the binary variables yTc and yTh. If $yTc = 1$, then the cold stream flows inside the inner tube, otherwise, $yTh = 1$, which is guaranteed by the following constraint:

$$yT_c + yT_h = 1 \quad (8)$$

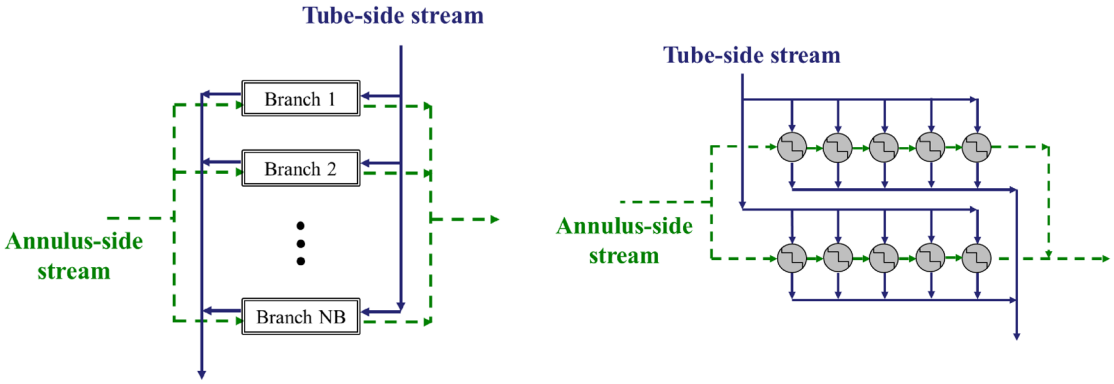

(a) General Structure

(b) Example with two branches (type III) (five units/branch)

Fig. 3 Multiple parallel branches. **a** General structure. **b** Example with two branches (type III) (five units/branch)

Structural constraints

The following constraint ensures that if the tube-side has more than one parallel passage, the annular side can be only arranged in series and vice-versa:

$$yPt_{sE=1} + yPa_{sE=1} \geq 1 \tag{9}$$

The following constraint guarantees that the outer tube's inner diameter is larger than the inner tube's outer diameter.

$$yd_{sd} + yD_{sD} \leq 1 \forall (sd, sD) \in SDD \tag{10}$$

where SDD is the set of forbidden (sd, sD) combinations.

Inner tube thermal and hydraulic modeling

The flow velocity inside the inner tube, its corresponding Reynolds number, and additional linear inequalities are:

$$vt = \sum_{sd=1}^{sdmax} \sum_{sB=1}^{sBmax} \sum_{sE=1}^{sEmax} \sum_{sST} \frac{4\widehat{m}_{sST}}{\pi \widehat{\rho}_{sST} \widehat{pdti}_{sd}^{2} \widehat{pNB}_{sB} \widehat{pNE}_{sE}} wvt_{sd,sB,sE,sST} \tag{11}$$

$$Ret = \sum_{sd=1}^{sdmax} \sum_{sB=1}^{sBmax} \sum_{sE=1}^{sEmax} \sum_{sST} \frac{4\widehat{m}_{sST}}{\pi \widehat{\mu}_{sST} \widehat{pdti}_{sd} \widehat{pNB}_{sB} \widehat{pNE}_{sE}} wvt_{sd,sB,sE,sST} \tag{12}$$

$$wvt_{sd,sB,sE,sST} \leq yd_{sd} \tag{13}$$

$$wvt_{sd,sB,sE,sST} \leq yB_{sB} \tag{14}$$

$$wvt_{sd,sB,sE,sST} \leq yPt_{sE} \tag{15}$$

$$wvt_{sd,sB,sE,sST} \leq yT_{sST} \tag{16}$$

$$wvt_{sd,sB,sE,sST} \geq yd_{sd} + yB_{sB} + yPt_{sE} + yT_{sST} - 3 \tag{17}$$

The Prandtl number of the inner tube stream becomes:

$$Prt = \frac{\widehat{Cp}_c \widehat{\mu}_c}{\widehat{k}_c} yT_c + \frac{\widehat{Cp}_h \widehat{\mu}_h}{\widehat{k}_h} yT_h \tag{18}$$

The evaluation of the Nusselt number by the Sieder & Tate correlation is now:

$$Nut^{S\&T} = \sum_{sB=1}^{sBmax} \sum_{sE=1}^{sEmax} \sum_{sLh=1}^{sLhmax} \sum_{sST} \widehat{pNut}_{sB,sE,sLh,sST}^{S\&T} wNut_{sB,sE,sLh,sST} \tag{19}$$

$$wNut_{sB,sE,sLh,sST} \leq yB_{sB} \tag{20}$$

$$wNut_{sB,sE,sLh,sST} \leq yPt_{sE} \tag{21}$$

$$wNut_{sB,sE,sLh,sST} \leq yLh_{sLh} \tag{22}$$

$$wNut_{sB,sE,sLh,sST} \leq yT_{sST} \tag{23}$$

$$wNut_{sB,sE,sLh,sST} \geq yB_{sB} + yPt_{sE} + yLh_{sLh} + yT_{sST} - 3 \tag{24}$$

where the parameter $\widehat{pNut}_{sB,sE,sLh,sST}^{S\&T}$ is given by:

$$\widehat{pNut}_{sB,sE,sLh,sST}^{S\&T} = 1.86 \left(\frac{8\widehat{Cp}_{sST} \widehat{m}_{sST}}{\pi \widehat{k}_{sST} \widehat{pNB}_{sB} \widehat{pNE}_{sE} \widehat{pLh}_{sLh}} \right)^{1/3} \tag{25}$$

The following equation allows the selection of the appropriate Re number using binary variables.

$$Ret \le 1311yRet_1 + 2300yRet_2 + 3380yRet_3 + \widehat{URey}Ret_4 \tag{26}$$

$$Ret \ge 1311yRet_2 + 2300yRet_3 + 3380yRet_4 + \varepsilon \tag{27}$$

$$Prt \le 5yPrt_1 + \widehat{UPry}Prt_2 \tag{28}$$

$$Prt \ge 5yPrt_2 + \varepsilon \tag{29}$$

$$Nut^{S\&T} \le 3.66yNut_1 + \widehat{UNuy}Nut_2 - \varepsilon \tag{30}$$

$$Nut^{S\&T} \ge 3.66yNut_2 \tag{31}$$

$$\sum_{sRet=1}^{sRetmax} yRet_{sRet} = 1 \tag{32}$$

$$yPrt_1 + yPrt_2 = 1 \tag{33}$$

$$yNut_1 + yNut_2 = 1 \tag{34}$$

The pressure drop in the tubes becomes:

$$\begin{aligned}\Delta Pt = &\sum_{sd=1}^{sdmax}\sum_{sB=1}^{sBmax}\sum_{sNh=1}^{sNhmax}\sum_{sE=1}^{sEmax}\sum_{sLh=1}^{sLhmax}\sum_{sE'=1}^{sEmax}\sum_{sST}\\ &\Big(\widehat{pdPt}1_{sd,sB,sE,sNh,sLh,sE',sST}wdPt_{sd,sB,sNh,sLh,sE,sE',sST,1}\\ &+\widehat{pdPt}23_{sd,sB,sE,sNh,sLh,sE',sST}wdPt_{sd,sB,sNh,sLh,sE,sE',sST,2}\\ &+\widehat{pdPt}23_{sd,sB,sE,sNh,sLh,sE',sST}wdPt_{sd,sB,sNh,sLh,sE,sE',sST,3}\\ &+\widehat{pdPt}4_{sd,sB,sE,sNh,sLh,sE',sST}wdPt_{sd,sB,sNh,sLh,sE,sE',sST,4}\Big)\end{aligned} \tag{35}$$

$$wdPt_{sd,sB,sE,sNh,sLh,sE',sST,sRet} \le wA_{sd,sB,sE,sNh,sLh,sE'} \tag{36}$$

$$wdPt_{sd,sB,sE,sNh,sLh,sE',sST,sRet} \le yT_{sST} \tag{37}$$

$$wdPt_{sd,sB,sE,sNh,sLh,sE',sST,sRet} \le yRet_{sRet} \tag{38}$$

$$wdPt_{sd,sB,sE,sNh,sLh,sE',sST,sRet} \ge wA_{sd,sB,sE,sNh,sLh,sE'} + yT_{sST} + yRet_{sRet} - 2 \tag{39}$$

The additional parameters inserted for simplification purposes in Eq. (35) are given by:

$$\widehat{pdPt}1_{sd,sB,sE,sNh,sLh,sE',sST} = \frac{128\hat{\mu}_{sST}\hat{m}_{sST}\widehat{pNh}_{sNh}\widehat{pLh}_{sLh}\widehat{pNE}_{sE'}}{\pi\hat{\rho}_{sST}\widehat{pdti}_{sd}^{4}\widehat{pNB}_{sB}\widehat{pNE}_{sE}} \tag{40}$$

$$\widehat{pdPt}23_{sd,sB,sE,sNh,sLh,sE',sST} = \frac{0.3904\hat{m}_{sST}^{2}\widehat{pNh}_{sNh}\widehat{pLh}_{sLh}\widehat{pNE}_{sE'}}{\pi^{2}\hat{\rho}_{sST}\widehat{pdti}_{sd}^{5}\widehat{pNB}_{sB}^{2}\widehat{pNE}_{sE}^{2}} \tag{41}$$

$$\begin{aligned}\widehat{pdPt}4_{sd,sB,sE,sNh,sLh,sE',sST} =&\frac{0.112\hat{m}_{sST}^{2}\widehat{pNh}_{sNh}\widehat{pLh}_{sLh}\widehat{pNE}_{sE'}}{\pi^{2}\hat{\rho}_{sST}\widehat{pdti}_{sd}^{5}\widehat{pNB}_{sB}^{2}\widehat{pNE}_{sE}^{2}}\\ &+\frac{4.719\hat{\mu}_{sST}^{0.42}\hat{m}_{sST}^{1.58}\widehat{pNh}_{sNh}\widehat{pLh}_{sLh}\widehat{pNE}_{sE'}}{\pi^{1.58}\hat{\rho}_{sST}\widehat{pdti}_{sd}^{4.58}\widehat{pNB}_{sB}^{1.58}\widehat{pNE}_{sE}^{1.58}}\end{aligned} \tag{42}$$

Annulus side thermal and hydraulic modeling

The annulus-side stream velocity, its corresponding Reynolds number, and additional linear inequalities are given by:

$$va = \sum_{sd=1}^{sdmax}\sum_{sD=1}^{sDmax}\sum_{sB=1}^{sBmax}\sum_{sE=1}^{sEmax}\sum_{sST}\frac{\hat{m}_{sST^*}}{\hat{\rho}_{sST^*}\widehat{pAa}_{sd,sD}\widehat{pNB}_{sB}\widehat{pNE}_{sE}}wva_{sd,sD,sB,sE,sST} \tag{43}$$

$$Rea = \sum_{sd=1}^{sdmax}\sum_{sD=1}^{sDmax}\sum_{sB=1}^{sBmax}\sum_{sE=1}^{sEmax}\sum_{sST}\frac{\hat{m}_{sST^*}\widehat{pdh}_{sd,sD}}{\hat{\mu}_{sST^*}\widehat{pAa}_{sd,sD}\widehat{pNB}_{sB}\widehat{pNE}_{sE}}wva_{sd,sD,sB,sE,sST} \tag{44}$$

$$wva_{sd,sD,sB,sE,sST} \le yd_{sd} \tag{45}$$

$$wva_{sd,sD,sB,sE,sST} \le yD_{sD} \tag{46}$$

$$wva_{sd,sD,sB,sE,sST} \le yB_{sB} \tag{47}$$

$$wva_{sd,sD,sB,sE,sST} \le yPa_{sE} \tag{48}$$

$$wva_{sd,sD,sB,sE,sST} \le yT_{sST} \tag{49}$$

$$wva_{sd,sD,sB,sE,sST} \ge yd_{sd} + yD_{sD} + yB_{sB} + yPa_{sE} + yT_{sST} - 4 \tag{50}$$

where if $sST = h$, then $sST^* = c$ and vice-versa.

The equations for the Prandtl number and the Nusselt numbers for the annulus-side stream become:

$$Pra = \frac{\widehat{Cp}_c\hat{\mu}_c}{\hat{k}_c}yT_h + \frac{\widehat{Cp}_h\hat{\mu}_h}{\hat{k}_h}yT_c \tag{51}$$

$$Nua^{S\&T} = \sum_{sd=1}^{sdmax}\sum_{sD=1}^{sDmax}\sum_{sB=1}^{sBmax}\sum_{sE=1}^{sEmax}\sum_{sLh=1}^{sLhmax}\sum_{sST} \widehat{pNua}^{S\&T}_{sd,sD,sB,sE,sLh,sST} wNua_{sd,sD,sB,sE,sLh.sST} \quad (52)$$

$$wNua_{sd,sD,sB,sE,sLh.sST} \le wva_{sd,sD,sB,sE,sST} \quad (53)$$

$$wNua_{sd,sD,sB,sE,sLh.sST} \le yLh_{sLh} \quad (54)$$

$$wNua_{sd,sD,sB,sE,sLh.sST} \ge wva_{sd,sD,sB,sE,sST} + yLh_{sLh} - 1 \quad (55)$$

where the parameter $\widehat{pNua}^{S\&T}_{sd,sD,sB,sE,sLh,sST}$ is given by:

$$\widehat{pNua}^{S\&T}_{sd,sD,sB,sE,sLh,sST} = 1.86\left(\frac{2\widehat{Cp}_{sST^*}\widehat{m}_{sST^*}\widehat{pdh}^{2}_{sd,sD}}{\widehat{k}_{sST^*}\widehat{pAa}_{sd,sD}\widehat{pNB}_{sB}\widehat{pNE}_{sE}\widehat{pLh}_{sLh}}\right)^{\frac{1}{3}} \quad (56)$$

where if $sST = h$, then $sST^* = c$ and vice-versa.

The constraints relating binary variables to Re ranges for the tube-side remain the same:

$$Rea \le 500yRea_1 + 2300yRea_2 + 10000yRea_3 + \widehat{URe}yRea_4 \quad (57)$$

$$Rea \ge 500yRea_2 + 2300yRea_3 + 10000yRea_4 + \varepsilon \quad (58)$$

$$Pra \le 5yPra_1 + \widehat{UPr}yPra_2 \quad (59)$$

$$Pra \ge 5yPra_2 + \varepsilon \quad (60)$$

$$Nua^{S\&T} \le 3.66yNua_1 + \widehat{UNu}yNua_2 - \varepsilon \quad (61)$$

$$Nua^{S\&T} \ge 3.66yNua_2 \quad (62)$$

$$\sum_{sRea=1}^{sReamax} yRea_{sRea} = 1 \quad (63)$$

$$yPra_1 + yPra_2 = 1 \quad (64)$$

$$yNua_1 + yNua_2 = 1 \quad (65)$$

The pressure drop of the flow in the annulus is given by

$$\Delta Pa = \sum_{sd=1}^{sdmax}\sum_{sD=1}^{sDmax}\sum_{sB=1}^{sBmax}\sum_{sE=1}^{sEmax}\sum_{sNh=1}^{sNhmax}\sum_{sLh=1}^{sLhmax}\sum_{sE'=1}^{sEmax}\sum_{sST} (\widehat{pdPa}1_{sd,sD,sB,sE,sNh,sLh,sE',sST} wdPa_{sd,sD,sB,sNh,sLh,sE.sE'sST,1} + \widehat{pdPa}23_{sd,sD,sB,sE,sNh,sLh,sE',sST}(wdPa_{sd,sD,sB,sNh,sLh,sE.sE'sST,2} + wdPa_{sd,sD,sB,sNh,sLh,sE.sE'sST,3}) + \widehat{pdPa}4_{sd,sD,sB,sE,sNh,sLh,sE',sST} wdPa_{sd,sD,sB,sNh,sLh,sE.sE'sST,4}) \quad (66)$$

$$wdPa_{sd,sD,sB,sE,sNh,sLh,sE',sST,sRea} \le wA_{sd,sB,sE,sNh,sLh,sE'} \quad (67)$$

$$wdPa_{sd,sD,sB,sNh,sLh,sE.sE'sST,sRea} \le yD_{sD} \quad (68)$$

$$wdPa_{sd,sD,sB,sNh,sLh,sE.sE'sST,sRea} \le yT_{sST} \quad (69)$$

$$wdPa_{sd,sD,sB,sNh,sLh,sE.sE'sST,sRea} \le yRea_{sRea} \quad (70)$$

$$wdPa_{sd,sD,sB,sNh,sLh,sE.sE'sST,sRea} \ge wA_{sd,sB,sNh,sLh,sE,sE'} + yD_{sD} + yT_{sST} + yRea_{sRea} - 3 \quad (71)$$

where:

$$\widehat{pdPa}1_{sd,sD,sB,sE,sNh,sLh,sE',sST} = \frac{32\widehat{\mu}_{sST^*}\widehat{m}_{sST^*}\widehat{pNh}_{sNh}\widehat{pLh}_{sLh}\widehat{pNE}_{sE}}{\widehat{\rho}_{sST^*}\widehat{pdh}^{2}_{sd,sD}\widehat{pAa}_{sd,sD}\widehat{pNB}_{sB}\widehat{pNE}_{sE'}} \quad (72)$$

$$\widehat{pdPa}23_{sd,sD,sB,sE,sNh,sLh,sE',sST} = \frac{0.01348\widehat{m}^{2}_{sST^*}\widehat{pNh}_{sNh}\widehat{pLh}_{sLh}\widehat{pNE}_{sE}}{\widehat{\rho}_{sST^*}\widehat{pdh}_{sd,sD}\widehat{pAa}^{2}_{sd,sD}\widehat{pNB}^{2}_{sB}\widehat{pNE}^{2}_{sE'}} + \frac{16.328\widehat{\mu}^{0.93}_{sST^*}\widehat{m}^{1.07}_{sST^*}\widehat{pNh}_{sNh}\widehat{pLh}_{sLh}\widehat{pNE}_{sE}}{\widehat{\rho}_{sST^*}\widehat{pdh}^{1.93}_{sd,sD}\widehat{pAa}^{1.07}_{sd,sD}\widehat{pNB}^{1.07}_{sB}\widehat{pNE}^{1.07}_{sE'}} \quad (73)$$

$$\widehat{pdPa}4_{sd,sD,sB,sE,sNh,sLh,sE',sST} = \frac{0.089\widehat{\mu}^{0.1865}_{sST^*}\widehat{m}^{1.8135}_{sST^*}\widehat{pNh}_{sNh}\widehat{pLh}_{sLh}\widehat{pNE}_{sE}}{\widehat{\rho}_{sST^*}\widehat{pdh}^{1.1865}_{sd,sD}\widehat{pAa}^{1.8135}_{sd,sD}\widehat{pNB}^{1.8135}_{sB}\widehat{pNE}^{1.8135}_{sE'}} \quad (74)$$

where if $sST = h$, then $sST^* = c$ and vice-versa.

Heat transfer rate equation

$$A = \sum_{sd=1}^{sdmax}\sum_{sB=1}^{sBmax}\sum_{sNh=1}^{sNhmax}\sum_{sLh=1}^{sLhmax}\sum_{sE=1}^{sEmax}\sum_{sE'=1}^{sE'max} \widehat{pA}_{sd,sB,sE,sNh,sLh,sE'} wA_{sd,sB,sE,sNh,sLh,sE'} \quad (75)$$

$$wA_{sd,sB,sNh,sLh,sE,sE'} \le yd_{sd} \quad (76)$$

$$wA_{sd,sB,sNh,sLh,sE,sE'} \le yB_{sB} \quad (77)$$

$$wA_{sd,sB,sNh,sLh,sE,sE'} \le yNh_{sNh} \quad (78)$$

$$wA_{sd,sB,sNh,sLh,sE,sE'} \le yLh_{sLh} \quad (79)$$

$$wA_{sd,sB,sNh,sLh,sE,sE'} \le yPt_{sE} \quad (80)$$

$$wA_{sd,sB,sNh,sLh,sE,sE'} \le yPa_{sE'} \tag{81}$$

$$wA_{sd,sB,sNh,sLh,sE,sE'} \ge yd_{sd} + yB_{sB} + yNh_{sNh} + yLh_{sLh} + yPt_{sE} + yPa_{sE'} - 5 \tag{82}$$

$$\widehat{pA}_{sd,sB,sNh,sLh,sE,sE'} = \pi \widehat{pNB}_{sB} \widehat{pNh}_{sNh} \widehat{pLh}_{sLh} \widehat{pNE}_{sE} \widehat{pNE}_{sE'} \tag{83}$$

The heat transfer rate, based on the LMTD method, after reformulation becomes:

$$\begin{aligned}
&\sum_{sd=1}^{sdmax} \sum_{sD=1}^{sDmax} \sum_{sB=1}^{sBmax} \sum_{sE=1}^{sEmax} \sum_{sLh=1}^{sLhmax} \sum_{sE'=1}^{sEmax} \sum_{sST} \\
&\Bigg[\sum_{sRet=1}^{2} \Bigg(\frac{\widehat{pdte}_{sd}}{\hat{k}_{sST} \widehat{pNut}^{theo}} wht^{theo}_{sd,sST,sRet,1,1} \\
&+ \frac{\widehat{pdte}_{sd}}{\hat{k}_{sST} \widehat{pNut}^{S\&T}_{sB,sE,sLh,sST}} wht^{S\&T}_{sd,sB,sLh,sE,sST,sRet,1,2} \\
&+ \frac{\widehat{pdte}_{sd}}{\hat{k}_{sST} \widehat{pNut}^{Hau}_{sB,sE,sLh,sST}} wht^{Hau}_{sd,sB,sLh,sE,sST,sRet,2} \Bigg) \\
&+ \frac{\widehat{pdte}_{sd}}{\hat{k}_{sST} \widehat{pNut}^{Gni}_{tran_{sd,sB,sE,sST}}} wht^{Gni}_{sd,sB,sE,sST,3} \\
&+ \frac{\widehat{pdte}_{sd}}{\hat{k}_{sST} \widehat{pNut}^{Gni}_{turb_{sd,sB,sE,sST}}} wht^{Gni}_{sd,sB,sE,sST,4} \\
&+ \widehat{Rf}_{sST} \frac{\widehat{pdte}_{sd}}{\widehat{pdti}_{sd}} wydT_{sd,sST} + \frac{\widehat{pdte}_{sd} \ln\left(\frac{\widehat{pdte}_{sd}}{\widehat{pdti}_{sd}}\right)}{2\widehat{ktube}} yd_{sd} \\
&+ \widehat{Rf}_{sST^*} yT_{sST} \\
&+ \sum_{sRea=1}^{2} \Bigg(\frac{\widehat{pdh}_{sd,sD}}{\hat{k}_{sST^*} \widehat{pNua}^{theo}} wha^{theo}_{sd,sD,sST,sRea,1,1} \\
&+ \frac{\widehat{pdh}_{sd,sD}}{\hat{k}_{sST^*} \widehat{pNua}^{S\&T}_{sd,sD,sB,sE',sLh,sST}} wha^{S\&T}_{sd,sD,sB,sE',sLh,sST,sRea,1,2} \\
&+ \frac{\widehat{pdh}_{sd,sD}}{\hat{k}_{sST^*} \widehat{pNua}^{Hau}_{sd,sD,sB,sE',sLh,sST}} wha^{Hau}_{sd,sD,sB,sLh,sE',sST,sRea,2} \Bigg) \\
&+ \frac{\widehat{pdh}_{sd,sD}}{\hat{k}_{sST^*} \widehat{pNua}^{Gni}_{tran_{sd,sD,sB,sE',sST}}} wha^{Gni}_{sd,sD,sB,sE',sST,3} \\
&+ \frac{\widehat{pdh}_{sd,sD}}{\hat{k}_{sST^*} \widehat{pNua}^{Gni}_{turb_{sd,sD,sB,sE',sST}}} wha^{Gni}_{sd,sD,sB,sE',sST,4} \Bigg] \\
&\le \frac{\widehat{\Delta Tlm}}{\left(\frac{\widehat{Aexc}}{100} + 1\right)} \sum_{sd=1}^{sdmax} \sum_{sB=1}^{sBmax} \sum_{sE=1}^{sEmax} \sum_{sNh=1}^{sNhmax} \sum_{sLh=1}^{sLhmax} \sum_{sE'=1}^{sE'max} \sum_{sST} \\
&(\widehat{pA}_{sd,sB,sNh,sLh,sE,sE'} wA_{sd,sB,sNh,sLh,sE,sE'} \\
&+ \widehat{pA}_{sd,sB,sNh,sLh,sE,sE'} \left(\widehat{pF}_{sST^*,sE} - 1\right) \\
&wAF_{sd,sB,sNh,sLh,sE,sE',sST} \\
&+ \widehat{pA}_{sd,sB,sNh,sLh,sE,sE'} \left(\widehat{pF}_{sST,sE'} - 1\right) \\
&wAF_{sd,sB,sNh,sLh,sE,sE',sST})
\end{aligned} \tag{84}$$

$$wydT_{sd,sST} \le yd_{sd} \tag{85}$$

$$wydT_{sd,sST} \le yT_{sST} \tag{86}$$

$$wydT_{sd,sST} \ge yd_{sd} + yT_{sST} - 1 \tag{87}$$

$$wht^{theo}_{sd,sST,sRet,1,1} \le wydT_{sd,sST} \text{for} sRet = \{1,2\} \tag{88}$$

$$wht^{theo}_{sd,sST,sRet,1,1} \le yRet_{sRet} \text{for} sRet = \{1,2\} \tag{89}$$

$$wht^{theo}_{sd,sST,sRet,1,1} \le yPrt_1 \text{for} sRet = \{1,2\} \tag{90}$$

$$wht^{theo}_{sd,sST,sRet,1,1} \le yNut_1 \text{for} sRet = \{1,2\} \tag{91}$$

$$wht^{theo}_{sd,sST,sRet,1,1} \ge wydT_{sd,sST} + yRet_{sRet} + yPrt_1 + yNut_1 - 3 \text{for} sRet = \{1,2\} \tag{92}$$

$$wht^{S\&T}_{sd,sB,sE,sLh,sST,sRet,1,2} \le wvt_{sd,sB,sE,sST} \text{for} sRet = \{1,2\} \tag{93}$$

$$wht^{S\&T}_{sd,sB,sE,sLh,sST,sRet,1,2} \le yLh_{sLh} \text{for} sRet = \{1,2\} \tag{94}$$

$$wht^{S\&T}_{sd,sB,sE,sLh,sST,sRet,1,2} \le yRet_{sRet} \text{for} sRet = \{1,2\} \tag{95}$$

$$wht^{S\&T}_{sd,sB,sE,sLh,sST,sRet,1,2} \le yPrt_1 \text{for} sRet = \{1,2\} \tag{96}$$

$$wht^{S\&T}_{sd,sB,sE,sLh,sST,sRet,1,2} \le yNut_2 \text{for} sRet = \{1,2\} \tag{97}$$

$$wht^{S\&T}_{sd,sB,sE,sLh,sST,sRet,1,2} \ge wvt_{sd,sB,sE,sST} + yLh_{sLh} + yRet_{sRet} + yPrt_1 + yNut_2 - 4 \text{for} sRet = \{1,2\} \tag{98}$$

$$wht^{Hau}_{sd,sB,sE,sLh,sST,sRet,2} \le wvt_{sd,sB,sE,sST} \text{for} sRet = \{1,2\} \tag{99}$$

$$wht^{Hau}_{sd,sB,sE,sLh,sST,sRet,2} \le yLh_{sLh} \text{for} sRet = \{1,2\} \tag{100}$$

$$wht^{Hau}_{sd,sB,sE,sLh,sST,sRet,2} \le yRet_{sRet} \text{for} sRet = \{1,2\} \tag{101}$$

$$wht^{Hau}_{sd,sB,sE,sLh,sST,sRet,2} \le yPrt_2 \text{for} sRet = \{1,2\} \tag{102}$$

$$wht^{Hau}_{sd,sB,sE,sLh,sST,sRet,2} \geq wvt_{sd,sB,sE,sST} + yLh_{sLh} + yRet_{sRet} + yPrt_2 - 3 \text{for} sRet = \{1,2\} \quad (103)$$

$$wht^{Gni}_{sd,sB,sE,sST,sRet} \leq wvt_{sd,sB,sE,sST} \text{for} sRet = \{3,4\} \quad (104)$$

$$wht^{Gni}_{sd,sB,sE,sST,sRet} \leq yRet_{sRet} \text{for} sRet = \{3,4\} \quad (105)$$

$$wht^{Gni}_{sd,sB,sE,sST,sRet} \geq wvt_{sd,sB,sE,sST} + yRet_{sRet} - 1 \text{for} sRet = \{3,4\} \quad (106)$$

$$wha^{theo}_{sd,sD,sST,sRea,1,1} \leq wydT_{sd,sST} \text{for} sRea = \{1,2\} \quad (107)$$

$$wha^{theo}_{sd,sD,sST,sRea,1,1} \leq yD_{sD} \text{for} sRea = \{1,2\} \quad (108)$$

$$wha^{theo}_{sd,sD,sST,sRea,1,1} \leq yRea_{sRea} \text{for} sRea = \{1,2\} \quad (109)$$

$$wha^{theo}_{sd,sD,sST,sRea,1,1} \leq yPra_1 \text{for} sRea = \{1,2\} \quad (110)$$

$$wha^{theo}_{sd,sD,sST,sRea,1,1} \leq yNua_1 \text{for} sRea = \{1,2\} \quad (111)$$

$$wha^{theo}_{sd,sD,sST,sRea,1,1} \geq wydT_{sd,sST} + yD_{sD} + yRea_{sRea} + yPra_1 + yNua_1 - 4 \text{for} sRea = \{1,2\} \quad (112)$$

$$wha^{S\&T}_{sd,sD,sB,sE',sLh,sST,sRea,1,2} \leq wva_{sd,sD,sB,sE',sST} \text{for} sRea = \{1,2\} \quad (113)$$

$$wha^{S\&T}_{sd,sD,sB,sE',sLh,sST,sRea,1,2} \leq yLh_{sLh} \text{for} sRea = \{1,2\} \quad (114)$$

$$wha^{S\&T}_{sd,sD,sB,sE',sLh,sST,sRea,1,2} \leq yRea_{sRea} \text{for} sRea = \{1,2\} \quad (115)$$

$$wha^{S\&T}_{sd,sD,sB,sE',sLh,sST,sRea,1,2} \leq yPra_1 \text{for} sRea = \{1,2\} \quad (116)$$

$$wha^{S\&T}_{sd,sD,sB,sE',sLh,sST,sRea,1,2} \leq yNua_2 \text{for} sRea = \{1,2\} \quad (117)$$

$$wha^{S\&T}_{sd,sD,sB,sE',sLh,sST,sRea,1,2} \geq va_{sd,sD,sB,sE',sST} + yLh_{sLh} + yRea_{sRea} + yPra_1 + yNua_2 - 4 \text{for} sRea = \{1,2\} \quad (118)$$

$$wha^{Hau}_{sd,sD,sB,sE',sLh,sST,sRea,2} \leq wva_{sd,sD,sB,sE',sST} \text{for} sRea = \{1,2\} \quad (119)$$

$$wha^{Hau}_{sd,sD,sB,sE',sLh,sST,sRea,2} \leq yLh_{sLh} \text{for} sRea = \{1,2\} \quad (120)$$

$$wha^{Hau}_{sd,sD,sB,sE',sLh,sST,sRea,2} \leq yRea_{sRea} \text{for} sRea = \{1,2\} \quad (121)$$

$$wha^{Hau}_{sd,sD,sB,sE',sLh,sST,sRea,2} \leq yPra_2 \text{for} sRea = \{1,2\} \quad (122)$$

$$wha^{Hau}_{sd,sD,sB,sE',sLh,sST,sRea,2} \geq wva_{sd,sD,sB,sE',sST} + yLh_{sLh} + yRea_{sRea} + yPra_2 - 3 \text{for} sRea = \{1,2\} \quad (123)$$

$$wha^{Gni}_{sd,sD,sB,sE',sST,sRea} \leq wva_{sd,sD,sB,sE',sST} \text{for} sRea = \{3,4\} \quad (124)$$

$$wha^{Gni}_{sd,sD,sB,sE',sST,sRea} \leq yRea_{sRea} \text{for} sRea = \{3,4\} \quad (125)$$

$$wha^{Gni}_{sd,sD,sB,sE',sST,sRea} \geq wva_{sd,sD,sB,sE',sST} + yRea_{sRea} - 1 \text{for} sRea = \{3,4\} \quad (126)$$

$$wAF_{sd,sB,sNh,sLh,sE,sE',sST} \leq wA_{sd,sB,sNh,sLh,sE,sE'} \quad (127)$$

$$wAF_{sd,sB,sNh,sLh,sE,sE',sST} \leq yT_{sST} \quad (128)$$

$$wAF_{sd,sB,sNh,sLh,sE,sE',sST} \geq wA_{sd,sB,sNh,sLh,sE,sE'} + yT_{sST} - 1 \quad (129)$$

where

$$\widehat{pNut}^{Hau}_{sB,sE,sLh,sST} = 3.66 + \frac{0.0668\left(\frac{8\widehat{Cp}_{sST}\widehat{m}_{sST}}{\pi\widehat{k}_{sST}\widehat{pNB}_{sB}\widehat{pNE}_{sE}\widehat{pLh}_{sLh}}\right)}{1 + 0.04\left(\frac{8\widehat{Cp}_{sST}\widehat{m}_{sST}}{\pi\widehat{k}_{sST}\widehat{pNB}_{sB}\widehat{pNE}_{sE}\widehat{pLh}_{sLh}}\right)^{2/3}} \quad (130)$$

$$\widehat{pNut}^{Gni}_{tran_{sd,sB,sE,sST}} = \frac{0.0061\left(\frac{4\widehat{m}_{sST}}{\pi\widehat{\mu}_{sST}\widehat{pdti}_{sd}\widehat{pNB}_{sB}\widehat{pNE}_{sE}} - 1000\right)\left(\frac{\widehat{Cp}_{sST}\widehat{\mu}_{sST}}{\widehat{k}_{sST}}\right)}{1 + 12.7(0.0061)^{\frac{1}{2}}\left(\left(\frac{\widehat{Cp}_{sST}\widehat{\mu}_{sST}}{\widehat{k}_{sST}}\right)^{\frac{2}{3}} - 1\right)} \quad (131)$$

$$\widehat{pNut}^{Gni}_{turb_{sd,sB,sE,sST}} = \frac{\left(0.00175 + 0.132\left(\frac{\pi\hat{\mu}_{sST}\widehat{pdti}_{sd}\widehat{pNB}_{sB}\widehat{pNE}_{sE}}{4\hat{m}_{sST}}\right)^{0.42}\right)\left(\frac{4\hat{m}_{sST}}{\pi\hat{\mu}_{sST}\widehat{pdti}_{sd}\widehat{pNB}_{sB}\widehat{pNE}_{sE}} - 1000\right)\left(\frac{\widehat{Cp}_{sST}\hat{\mu}_{sST}}{\hat{k}_{sST}}\right)}{1 + 12.7\left(0.00175 + 0.132\left(\frac{\pi\hat{\mu}_{sST}\widehat{pdti}_{sd}\widehat{pNB}_{sB}\widehat{pNE}_{sE}}{4\hat{m}_{sST}}\right)^{0.42}\right)^{1/2}\left(\left(\frac{\widehat{Cp}_{sST}\hat{\mu}_{sST}}{\hat{k}_{sST}}\right)^{\frac{2}{3}} - 1\right)} \tag{132}$$

$$\widehat{pNua}^{Hau}_{sd,sD,sB,sE,sLh,sST} = 3.66 + \frac{0.0668\frac{2\widehat{Cp}_{sST*}\hat{m}_{sST*}\widehat{pdh}^{2}_{sd,sD}}{\hat{k}_{sST*}\widehat{pAa}_{sd,sD}\widehat{pNB}_{sB}\widehat{pNE}_{sE}\widehat{pLh}_{sLh}}}{1 + 0.04\left(\frac{2\widehat{Cp}_{sST*}\hat{m}_{sST*}\widehat{pdh}^{2}_{sd,sD}}{\hat{k}_{sST*}\widehat{pAa}_{sd,sD}\widehat{pNB}_{sB}\widehat{pNE}_{sE}\widehat{pLh}_{sLh}}\right)^{\frac{2}{3}}} \tag{133}$$

$$\widehat{pNua}^{Gni}_{tran_{sd,sD,sB,sE,sST}} = \frac{\left(0.00337 + 4.082\left(\frac{\hat{\mu}_{sST*}\widehat{pAa}_{sd,sD}\widehat{pNB}_{sB}\widehat{pNE}_{sE}}{\hat{m}_{sST*}\widehat{pdh}_{sd,sD}}\right)^{0.93}\right)\left(\frac{\hat{m}_{sST*}\widehat{pdh}_{sd,sD}}{\hat{\mu}_{sST*}\widehat{pAa}_{sd,sD}\widehat{pNB}_{sB}\widehat{pNE}_{sE}} - 1000\right)\frac{\widehat{Cp}_{sST*}\hat{\mu}_{sST*}}{\hat{k}_{sST*}}}{1 + 12.7\left(0.00337 + 4.082\left(\frac{\hat{\mu}_{sST*}\widehat{pAa}_{sd,sD}\widehat{pNB}_{sB}\widehat{pNE}_{sE}}{\hat{m}_{sST*}\widehat{pdh}_{sd,sD}}\right)^{0.93}\right)^{\frac{1}{2}}\left(\left(\frac{\widehat{Cp}_{sST*}\hat{\mu}_{sST*}}{\hat{k}_{sST*}}\right)^{\frac{2}{3}} - 1\right)} \tag{134}$$

$$\widehat{pNua}^{Gni}_{turb_{sd,sD,sB,sE,sST}} = \frac{\left(0.02225\left(\frac{\hat{\mu}_{sST*}\widehat{pAa}_{sd,sD}\widehat{pNB}_{sB}\widehat{pNE}_{sE}}{\hat{m}_{sST*}\widehat{pdh}_{sd,sD}}\right)^{0.1865}\right)\left(\frac{\hat{m}_{sST*}\widehat{pdh}_{sd,sD}}{\hat{\mu}_{sST*}\widehat{pAa}_{sd,sD}\widehat{pNB}_{sB}\widehat{pNE}_{sE}} - 1000\right)\frac{\widehat{Cp}_{sST*}\hat{\mu}_{sST*}}{\hat{k}_{sST*}}}{1 + 12.7\left(0.02225\left(\frac{\hat{\mu}_{sST*}\widehat{pAa}_{sd,sD}\widehat{pNB}_{sB}\widehat{pNE}_{sE}}{\hat{m}_{sST*}\widehat{pdh}_{sd,sD}}\right)^{0.1865}\right)^{\frac{1}{2}}\left(\left(\frac{\widehat{Cp}_{sST*}\hat{\mu}_{sST*}}{\hat{k}_{sST*}}\right)^{\frac{2}{3}} - 1\right)} \tag{135}$$

where if $sST = h$, then $sST^{*} = c$ and vice-versa.

Pressure drop and velocity bounds

Bounds on flow velocity and pressure drop are given by:

$$vt \geq \hat{vt}_{min} \tag{136}$$

$$vt \leq \hat{vt}_{max} \tag{137}$$

$$va \geq \hat{va}_{min} \tag{138}$$

$$va \leq \hat{va}_{max} \tag{139}$$

$$\Delta Pt \leq \widehat{\Delta P}_{cdisp} yT_{c} + \widehat{\Delta P}_{hdisp} yT_{h} \tag{140}$$

$$\Delta Pa \leq \widehat{\Delta P}_{cdisp} yT_{h} + \widehat{\Delta P}_{hdisp} yT_{c} \tag{141}$$

Objective function

The objective function is given by the heat transfer area and a penalty term associated to the number of hairpins; thus, in case of equivalent solutions, the one with smaller number of elements is preferred:

$$\min A + \sum_{sNh=1}^{sNhmax} \widehat{php}\widehat{Nh}_{sNh} yNh_{sNh} \tag{142}$$

Solution of the optimization problem

The mathematical transformations techniques applied to generate the linear model imply a large increase in the number of constraints and variables. If the number of discrete alternatives of the search space is too high, the dimension of the MILP problem may be not able to be solved using a conventional PC. For example, the proposed linear formulation to the problems presented in Peccini et al. (2019) yields a MILM with 1,467,771,040 constraints and 300,784,517 variables.

This computational obstacle can be overcome using different approaches. The simpler is just to analyze the nature

of the design problem and select a limited number of discrete alternatives for the definition of the search space (the search space of Peccini et al. (2019), valid for various examples, could be limited according to the nature of each example). Another approach is to use parallel computing, where the original search space would be split into smaller ones by parametrization of discrete variables and solved simultaneously in several cores. During the run, every incumbent found would be broadcasted to the other core and allowing an update of the common upper bound.

Instead of the above alternatives, we introduce a novel approach: Smart enumeration of a parametrized search space. Thus, the global optimum can be obtained by solving a set of smaller MILP problems, either in series or in parallel, as described above. However, our novel contribution is that the parametrization allows the use of Smart Enumeration (Costa and Bagajewicz 2019), once a lower bound of the objective function is developed. We explain this procedure below.

Search space parameterization

As described above, we choose a few variables and use them as parameters. This reduces the number of variables and constraints generated during the reformulation. The new parametrized MILM can be solved using the subset of the decision variables that are left. To solve the entire problem, one has to repeat the optimization sequentially or in parallel, to cover the entire domain of the combinations of different values of the parameters. Figure 4 illustrates a representation of this procedure where a single large MILP problem is split into 9 smaller MILP problems. Each small MILP problem corresponds to a given set of combination of discrete values of the variables chosen for parametrization.

Different alternatives of parameters and variables were tested and the option with the best performance was the one where the structural variables (NB_{sB}, Nh_{sNh}, $NPt_{sE,}$ and NPa_{sE}) are transformed into parameters. Solving this new parametrized MILM with a MILP approach renders the best possible values of fluid allocation, diameters, and length. A comparison of this approach with other alternatives of groups of parameters and variables is displayed in the Supplementary Information (Sections S2, S3 and S4).

Based on this approach, the global optimum can be attained by solving the MILP for each possible combination of structural variables, i.e. an exhaustive enumeration. However, as discussed below, a smart enumeration procedure can reduce this computational effort, avoiding testing all combinations, but still attaining the global optimum. The Smart enumeration depends on the set up of a lower bound of the objective function of the parametrized MILP problem, as shown below.

Lower bound of the objective function

As discussed above, each solution candidate based on the parametrization of the search space corresponds to a set of discrete values of NB_{sB}, Nh_{sNh}, $NPt_{sE,}$ and NPa_{sE}. These are the combinations of the variables turned into parameters. The lower bound of the objective function of these solution candidates corresponds to the heat transfer area of the exchanger evaluated using the smallest values of the inner tube diameter and tube length, i.e. the lower bound of the heat transfer area is calculated using an inner tube diameter equal to $\min(\widehat{pdte}_{sd})$ and a hairpin tube length equal to $\min(\widehat{pLh}_{sLh})$ associated with the parametrized values of the candidate in relation to the the number of hairpins per unit, the number of parallel branches, and the number of units aligned in parallel in each branch for the tube-side and the annulus-side streams.

Smart enumeration

Smart Enumeration is based on the enumeration using a candidate ordering by the lower bound of the objective function that, associated with a proper stop criterion involving the objective function of the incumbent (upper bound), promotes a reduction of the computational effort, but still guaranteeing global optimality.

Then, one can order the enumeration options in ascending order of lower bounds so that the first structure tested is the one with the smaller lower bound and so on. The first viable solution found is saved as an incumbent, and during the enumeration, the incumbent is updated every time a better solution is found. Since the enumeration options

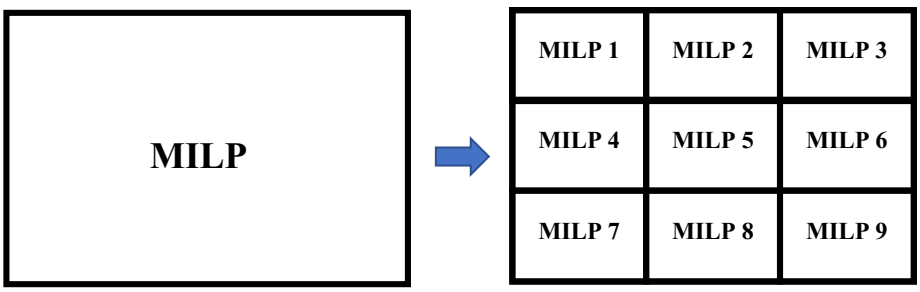

Fig. 4 Representation of the search space parametrization

are ordered in ascending order of lower bound, the gap between the incumbent and the lower bound decreases until the lower bounds of the remaining solutions become higher than the incumbent. At that point, the search is interrupted, for it is guaranteed that no other structure has a viable solution that would render a smaller area than that of the incumbent solution.

An extended version of the Smart Enumeration is proposed where each MILP problem is solved using an additional upper bound constraint associated with the incumbent heat exchanger area, for there is no interest in finding a higher area.

Results

The performance of the proposed approaches is illustrated by its application to four different examples, originally presented by Peccini et al. (2019). The flow velocities must be between 1 and 3 m/s, the pipe thermal conductivity is 16.27 W/(m °C) for Example 1 and 55 W/(m °C) for Examples 2 to 4, and the minimum excess area is 10% for Examples 1 and 4 and 20% for Examples 2 and 3. The details of all examples are displayed in the Supplementary Information (Section S3). All computational times reported here are associated to the solution of the MILP problems using the solver CPLEX in GAMS 24.7.1 running on an AMD Ryzen 9 3900X 12-Core Processor.

Table 1 displays the heat transfer area associated to the globally optimal results. The different services of the four examples are evidenced by the different optimal heat exchanger areas (that range from 1.84 to 88.73 m^2). The details of all solutions are presented in the Supplementary Information (Section S5).

Table 1 Globally optimal solutions for Examples 1 to 4

Variable	Example 1	Example 2	Example 3	Example 4
Total heat exchanger area (m^2)	9.19	1.84	88.73	40.86

Smart enumeration

The computational efficiency of the Smart Enumeration procedures is illustrated in Table 2, which displays the corresponding elapsed times.

The original Smart Enumeration enables a significant reduction in the number of enumerated candidates and consequently of the computational effort. This reduction is particularly intense in Example 2 (97.8%), where the optimal solution corresponds to a small heat exchanger that is found earlier, thus avoiding a long search. This large reduction pattern will always be repeated if the optimal solution has a small area compared with the other candidates of the search space.

The Extended Smart Enumeration does not change the number of MILP solved compared with Straight Smart Enumeration, but it does accelerate the convergence of the individual MILP problems and therefore reduces the total computational effort.

These results draw attention to the oversized search space employed in Peccini et al (2019), with areas ranging from 0.1022 to 9728.8 m^2, aimed to encompass different examples solutions. A tighter search domain would require less computational time (e.g. Example 3 solved for a reduced domain with Extended Smart Enumeration renders an elapsed time of only 194.1 s—see Supplementary Information, Table S4).

Conclusions

The mixed-integer linear programming problem proposed was successfully formulated through mathematical transformation techniques applied to a previously mixed-integer nonlinear model. The mathematically equivalent model does not show any convergence problems observed in nonlinear formulations, does not require any initial values as a starting point, and also presents the important advantage of guaranteeing global optimality. Therefore, the proposed procedure allows attaining the global optimum of the design problem using conventional MILP solvers, which are robust and widely available (there are even free codes, such as GLPK), thus avoiding the use of specialized global

Table 2 Elapsed time (s) with exhaustive and smart enumeration

Enumeration		Example 1	Example 2	Example 3	Example 4
Exhaustive	Total elapsed time (s)	3976.3	4542.7	5357.4	4766.2
	Enumerated candidates	7800	7800	7800	7800
Smart	Total elapsed time (s)	736.3	183.6	4155.9	2594.0
	Enumerated candidates	1217	167	5842	4002
Extended smart	Total elapsed time (s)	731.0	172.2	4043.5	2293.7
	Enumerated candidates	1217	167	5842	4002

nonlinear optimization solvers, which may be expensive and sometimes may fail to find initial feasible solutions or take a long time.

The problem size increases substantially for the MILP problem as compared with the previously proposed MINLP, rendering increased computational effort. This obstacle is handled by the proposition of an enumeration procedure, which substitutes the need to solve a large MILP problem with the solution of a limited set of smaller MILP problems. This procedure involves the parametrization of the search space and the establishment of a lower bound of the objective function for each smaller resultant MILP problem. The exploration of the search space through an ascending order of their lower bounds allows a reduction of the computational effort to identify the global optimum solution.

Solution obstacles related to large size MILP problems also occur in several other optimization applications, such as process scheduling (Floudas and Lin 2005), heat exchanger network synthesis (Chen et al. 2015), cogeneration systems (Lin et al. 2016), etc. Therefore the proposed approach for handling large size MILP problems can be an interesting alternative for other fields of applications.

Supplementary Information The online version contains supplementary material available at https://doi.org/10.1007/s43153-022-00238-2.

Acknowledgements André L. H. Costa would like to thank the National Council for Scientific and Technological Development (CNPq) for the research productivity fellowship (Process 310390/2019-2) and the Rio de Janeiro State University through the Prociência Program. Miguel J. Bagajewicz would like to thank the Rio de Janeiro State University (UERJ) for its scholarship of Visiting Researcher—PAPD Program and the financial support of the Federal University of Rio de Janeiro (UFRJ), through a visiting professor contract.

Author contributions AP: Conceptualization, Investigation, Methodology, Software, Validation, Visualization, Writing—original draft, Writing—review and editing. MB: Conceptualization, Investigation, Methodology, Supervision, Writing—original draft, Writing—review and editing. AC: Conceptualization, Formal Analysis, Funding acquisition, Investigation, Methodology, Project administration, Supervision, Writing—original draft, Writing—review and editing.

Funding This paper received financial support from the following institutions: National Council for Scientific and Technological Development (CNPq): Process 310390/2019-2, Rio de Janeiro State University (UERJ): Prociência Program and PAPD Program.

Availability of data and material All the data associated with the current paper are present in the text or the Supplementary Information file.

Code availability The code will be supplied upon request to the corresponding author.

Declarations

Conflict of interest On behalf of all authors, the corresponding author states that there is no conflict of interest.

References

Arjmandi H, Amiri P, Pour MS (2020) Geometric optimization of a double pipe heat exchanger with combined vortex generator and twisted tape: a CFD and response surface methodology (RSM) study. Therm Sci Eng Prog 18:100514

Chen Y, Grossmann IE, Miller DC (2015) Computational strategies for large-scale MILP transshipment models for heat exchanger network synthesis. Comp Chem Eng 82:68–83

Costa ALH, Bagajewicz MJ (2019) 110th Anniversary: on the departure from heuristics and simplified models toward globally optimal design of process equipment. Ind Eng Chem Res 58:18684–18702

Dastmalchi M, Sheikhzadeh GA, Arefmanesh A (2017) Optimization of micro-finned tubes in double pipe heat exchangers using particle swarm algorithm. Appl Therm Eng 119:1–9

Floudas CA, Lin X (2005) Mixed integer linear programming in process scheduling: modeling, algorithms, and applications. Ann Oper Res 139:131–162

Guy AR (2008) In: Hewitt G (ed) Heat exchanger design handbook. Begell House, New York

Han H, Bing-Xi L, Wu H, Shao W (2015) Multi-objective shape optimization of double pipe heat exchanger with inner corrugated tube using RSM method. Int J Therm Sci 90:173–186

Incropera FP, Dewitt DP (2007) Fundamentals of heat and mass transfer. John Wiley & Sons, New York

Iqbal Z, Syed KS, Ishaq M (2011) Optimal convective heat transfer in double pipe with parabolic fins. Int J Heat Mass Transf 54:5415–5426

Iqbal Z, Syed KS, Ishaq M (2013) Optimal fin shape in finned double pipe with fully developed laminar flow. Appl Therm Eng 51:1202–1223

Kakaç S, Liu H (2002) Heat exchangers selection, rating and thermal design. CRC Press, Boca Raton

Kola PVKV, Pisipaty SK, Mendu SS, Ghosh R (2021) Optimization of performance parameters of a double pipe heat exchanger with cut twisted tapes using CFD and RSM. Chem Eng Process 163:108362

Kumar S, Dinesha P (2021) Application of soft computing techniques to optimize thermal parameters in a double heat exchanger with cylindrical turbulators. Heat Transf 50:5286–5303

Lin F, Leyffer S, Munson T (2016) A two-level approach to large mixed-integer programs with application to cogeneration in energy-efficient buildings. Comput Optim Appl 65:1–46

Moloodpoor M, Mortazavi A, Özbalta N (2021) Thermo-economic optimization of double-pipe heat exchanger using a compound swarm intelligence. Heat Transf Res 52:1–20

Nahes ALM, Bagajewicz MJ, Costa ALH (2019) Design optimization of double-pipe heat exchangers using a discretized model. Ind Eng Chem Res 60:17611–17625

Peccini A, Lemos JC, Costa ALH, Bagajewicz MJ (2019) Optimal design of double pipe heat exchanger structures. Ind Eng Chem Res 58:12080–12096

Sahiti N, Krasniqi F, Fejzullahu X, Bunjaku J, Muriqi A (2008) Entropy generation minimization of a double-pipe pin fin heat exchanger. Appl Therm Eng 28:2337–2344

Saunders EAD (1988) Heat exchangers selection, design and construction. John Wiley & Sons, New York

Serth RW (2007) Process heat transfer principles and applications. Academic Press, Burlington

Söylemez MS (2004) Thermoeconomical optimization of double-pipe heat exchanger for waste heat recovery. J Thermophys 18:559–563

Sruthi B, Sasidhar A, Kumar AS, Sahu MK (2021) Comparative analysis of corrugation effect on thermohydraulic performance of double-pipe heat exchangers. Heat Transf 50:4522–4642

Swamee PK, Aggarwal N, Aggarwal V (2008) Optimum design of double pipe heat exchanger. Int J Heat Mass Transf 51:2260–2266

Syed KS, Iqbal Z, Ishaq M (2011) Optimal configuration of finned annulus in a double pipe with fully developed laminar flow. Appl Therm Eng 31(1435):1446

Xie JH, Cui HC, Liu ZC, Liu W (2022) Optimization design of helical micro fin tubes based on exergy destruction minimization principle. Appl Therm Eng 200:117640